International Journal on Interactive Design and Manufacturing (IJIDeM)
https://doi.org/10.1007/s12008-024-02167-5

ORIGINAL ARTICLE

Design and development of a quadruped ladder climbing robot using optimized PID parameters using genetic algorithm

Darshita Shah[1] · Jatin Dave[1] · Devarshi Dave[1] · Shivam Soni[1] · Kaushik Patel[1]

Received: 12 May 2023 / Accepted: 1 November 2024

Abstract

This paper presents a design and analysis of a ladder-climbing robot that can climb ladders attached to telecom towers. Telecommunication tower ladders are kept perfectly vertical at 90^0. The design of a robot is carried out concerning dynamic stability. The design resembles a quadrupedal climbing robot whose biomimetic climbing movement is the monkey climbing pattern. The paper includes kinematic, dynamic, finite element analysis and motion simulation of the proposed robot. It also presents the optimization using an evolutionary genetic algorithm for PID parameters to ensure the stable motion of a robot on the vertical ladder. The dynamic analysis results provide the actuator's torque that supports the selection of the actuators. Using tuned PID controller parameters with optimized values smoothens the robot's motion and reduces jerks. The developed robot shows satisfactory climbing motion on the ladder of the tower.

✉ Jatin Dave
jatin.dave@nirmauni.ac.in

[1] Mechanical Engineering Department, Institute of Technology, Nirma University, Ahmedabad, India

Published online: 08 December 2024

Graphic abstract

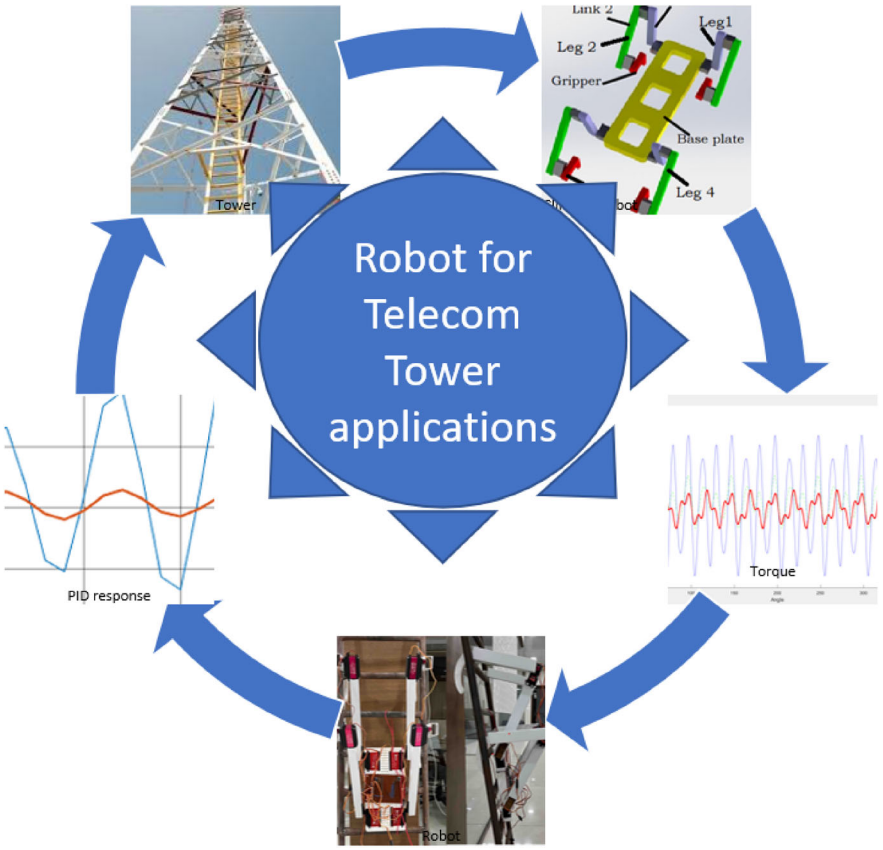

Keywords Quadruped robot · Forward kinematics · Inverse kinematics · Dynamic analysis · Trajectory planning · Genetic algorithm · PID controller

Abbreviations

${}^{i-1}T_i$	Homogeneous transformation matrix of (i-1)th and ith axis
c_1	$\text{Cos}\theta_1$
s_1	$\text{Sin}\theta_1$
c_2	$\text{Cos}\theta_2$
s_2	$\text{Sin}\theta_2$
c_{12}	$\text{Cos}\ (\theta_1 + \theta_2)$
s_{12}	$\text{Sin}\ (\theta_1 + \theta_2)$
c_{123}	$\text{Cos}(\theta_1 + \theta_2 + \theta_3)$
s_{123}	$\text{Cos}(\theta_1 + \theta_2 + \theta_3)$
$\lvert\Delta f\rvert$	Difference of maximum and minimum error
t	Time
Ii	Mass moment of Inertia of the link, where $i = 1, 2, 3$
Ci	Damping property of the material, where $i = 1, 2, 3$
Ki	Stiffness of the material, where $i = 1, 2, 3$
Tfi	Transfer function of the system, where $i = 1, 2, 3$
Ki	Kinetic energy, where $i = 1, 2, 3$
K	$1/2*M*V^2$ (Where M and V are the elemental mass and velocity)
Pi	Potential Energy, where $i = 1, 2, 3$
P	$M * G * Y$ (Where Y is the elemental displacement)

1 Introduction

The invention of the mobile phone and advancement in telecom technology has changed the perspectives of human life in the last two decades. The telecommunication industry is vital for social communication, national security, and connectivity 24 × 7 × 365. An increase in the demand for communication payload increases the demand for more network towers and supporting infrastructure [1]. During the COVID-19 pandemic, we have nothing but only mobile connectivity. All activities converted to online mode, and

telecommunication networks helped to deal with adverse situations [2, 3]. Connectivity device utilization has become very common, and demand for it is increasing daily. To support this, robust network connectivity is important. The growth in the number of telecom network towers worldwide with the connectivity demand is obvious. According to a survey, the global telecommunications tower market is projected to grow at an 18.0% annualized growth rate over the forecast period 2018–2025 [4–7]. Telephone companies face difficulties maintaining such a massive network of telecom towers as work-at-height hazards are prominent. The majority of the telecom tower maintenance work includes work at height. The risks associated with working at heights are radiation, falls from towers, electric shocks and insect bites. The mobile communication tool is becoming necessary for people in the present scenario [8]. The network tower maintenance task has become more crucial with the advancement of technology like 2G, 3G, 4G, and now 5G. It is possible to incorporate robots in the field of telecommunications tower maintenance, which can assist the tower maintenance team [9, 10]. A climbing robot can support dangerous work situations and bring a green technological solution. Robots find their application when the task is repetitive in nature and in a dangerous working environment for human beings [11–14]. One such application is the field maintenance of telecom network towers.

The maintenance of telecommunications towers is carried out manually worldwide by qualified Riggers (certified tower climbers). Riggers are used to maintain telecom towers, and the major part of their job is to perform maintenance at the top of the tower in all environmental situations [15–19]. They become victims of work-at-height hazards. These include falling from heights, exposure to radiation, bird strikes, insect bites and electrical shocks. In addition, they are expected to wear a tool bag weighing 7–8 kg while climbing. Their climbing frequency varies from 12 to 18 times per day per rigger [20, 21]. Telecom infrastructure provider companies are worried about the fatality and loss of time injury data. The deployment of robots to assist the workers in telecom tower maintenance is required for the long-term sustainability of network tower maintenance.

The authors of this article have surveyed to judge the requirements of the robotics and automation system for the field maintenance of towers. Expert opinion from the telecom field is important to consider while designing a robot to maintain a telecom tower. Shah and Dave presented a descriptive analysis of the robotic system requirements [22]. According to the expert view, a compact robot with data collation and storage system for inspection is desired. It is easy to operate and transport from one site to another.

The field of climbing robots is of great interest to the researcher. An exhaustive literature review is conducted to design a climbing robot capable of climbing telecom towers. The climbing robot presented by Tavakoli et al. is a two-jaw gripper pipe climbing robot [23]. Pipe, pole, structure, uneven surfaces climbing robots consist of wheeled, gripping jaws, magnetic or vacuum adhesion system [24, 25]. Few climbing robots are based on biomimetics inspired by snakes, lizards, alligators and spiders [26–29]. For the application of telecom towers, it is necessary to identify the present climbing arrangements the riggers use as part of their routine tower climbing job [30–35]. All types of telecom towers contain a ladder attached to them for climbing. These ladders are kept perfectly vertical to the ground. The robot can climb on the same ladder. The literature supporting vertical ladder climbing is surveyed, and its key features are identified [36–39]. Figure 1 shows the ladder-climbing robot in research and development. Figures 1a and b show the ladder climbing robot with 5 degrees of freedom on each leg and bulky controllers mounted on the base of a quadruped robot. Figure 1c shows the three contact points hexapod robot Asterisk to climb the vertical ladder. Figure 1d and e represent the humanoid robots following a three-point contact climbing gait pattern.

Robots are designed and analysed for climbing walls and surfaces and transition between wall and ground surfaces. The ladder-climbing robots developed so far are for some intended purpose and specialized applications. Their degrees of freedom are pretty high; they contain complicated control mechanisms and use humanoid gait planning patterns. It makes them costly, bulky and difficult to control [40–44]. For the climbing telecom tower's ladder application, the silent features must be considered: space, weight, stability, payload and cost. Compared to two-point-of-contact gait patterns, three-point gait is more stable on vertical ladders, which also carries a high payload. A three-point-of-contact gait quadruped climbing robot is designed and developed for the telecom tower's application. The authors have designed a compact, easy-to-operate robot that adheres to the dimensions of ladders and telecom towers with lesser degrees of freedom.

The primary design consideration is the robot to be accommodated in a narrow tower space; as the tower's cross-section area narrows at height. With lesser degrees of freedom, robots need fewer actuators that can be easily controlled and operated with reduced cost. The proposed design is high-strength, can carry the required payload and perform stable vertical ladder climbing.

This paper presents the design and analysis of robot, optimization of controlling parameters and development of a ladder-climbing robot. The methodology for addressing the problem is shown in Fig. 2. It is necessary to conceptualize a robot's design that may climb the telecommunications tower's ladder. Certain specific parameters taken into account at the conceptualization stage are the size of a robot, the adhesion mechanism on the ladder, and the strength and payload

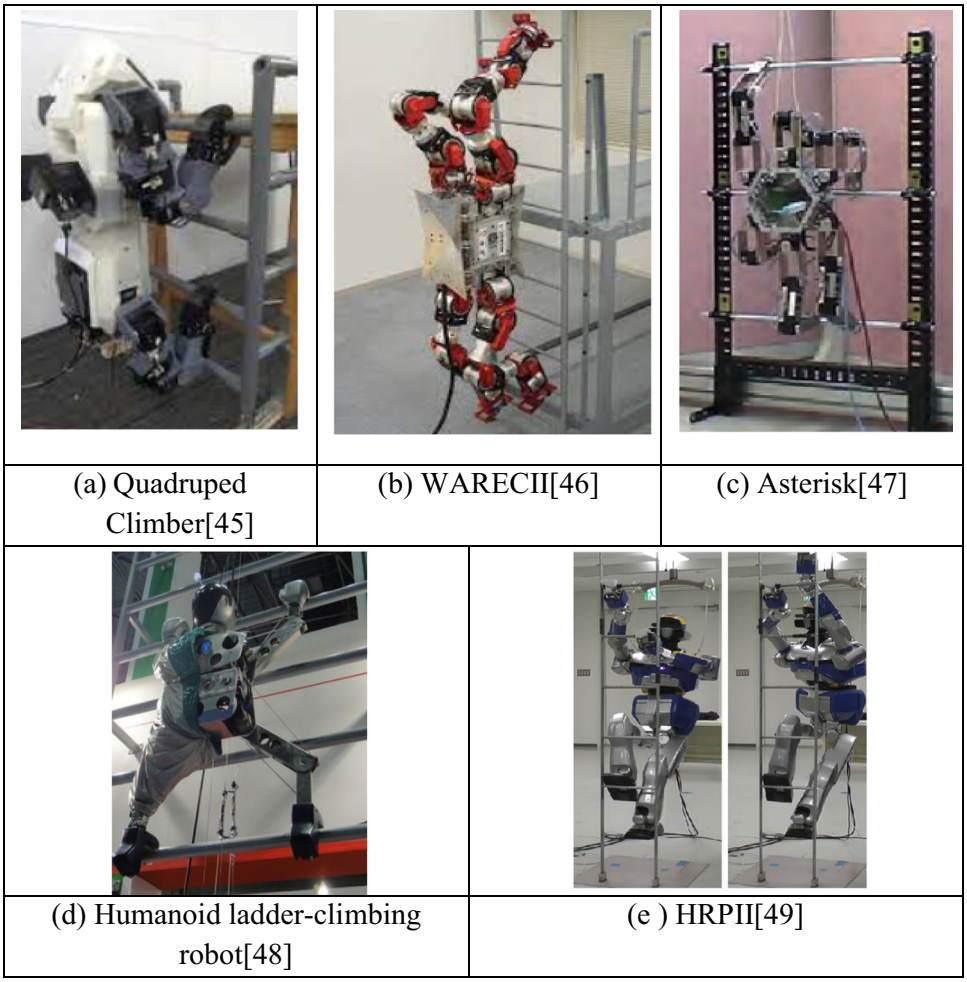

Fig. 1 Ladder climbing robots in research and development a quadruped climber [45], **b** WARECII [46] **c** asterisk [47] **d** humanoid ladder-climbing robot [48] **e** HRPII [49]

of the robot. Compact design and large payload capacity are essential parameters. The ladders are maintained vertically, so the robot's stability during the movement is very important. The design of a gripper shall be such that contact with the ladder rung remains correct.

Motion simulation is performed in solid works to visualize the upward motion of the climbing robot. The mathematical equations developed are coded, and the results of the kinematic and dynamic parameters are obtained and plotted for interpretation. Finite element analysis results are obtained for induced stresses and deformations. The dynamic stability of the robot is an important parameter, and tuning the PID controller parameters like a proportional, derivative, and integral gain for stable motion is recommended. An evolutionary Genetic Algorithm is used for PID parameters tuning, and ITAE (Integral Time Absolute Error) minimization is carried out [50–52]. Considering the results of dynamic analysis actuators are selected for the development of the robot. The Experimental trials of the developed prototype are conducted, and stable ladder climbing motion is achieved. The quadruped design robot has four legs, each with 3 degrees of freedom. The total DOF of a robot is 12, and all the joints are revolute. The inspiration for the design is based on the climbing movement of apes.

The rest of the paper is organized as follows. The biomechanical design of a robot is presented in Sect. 2, along with the types of towers and ladder information. The mechanical elements are conceived according to basic mathematical considerations. An accurate mathematical formulation is important for the desired movement. The Forward, inverse kinematics, finite element analysis, motion simulation and dynamic analysis are presented in Sect. 3. Section 4 presents the results of the Optimization of PID parameters. The experiment on climbing the ladder is given in Sect. 5. The concluding remarks are given in Sect. 6 of this article.

2 Design of quadruped ladder climbing robot

This section includes the proposed robot's design to climb the ladder attached to the telecom tower. It is important to

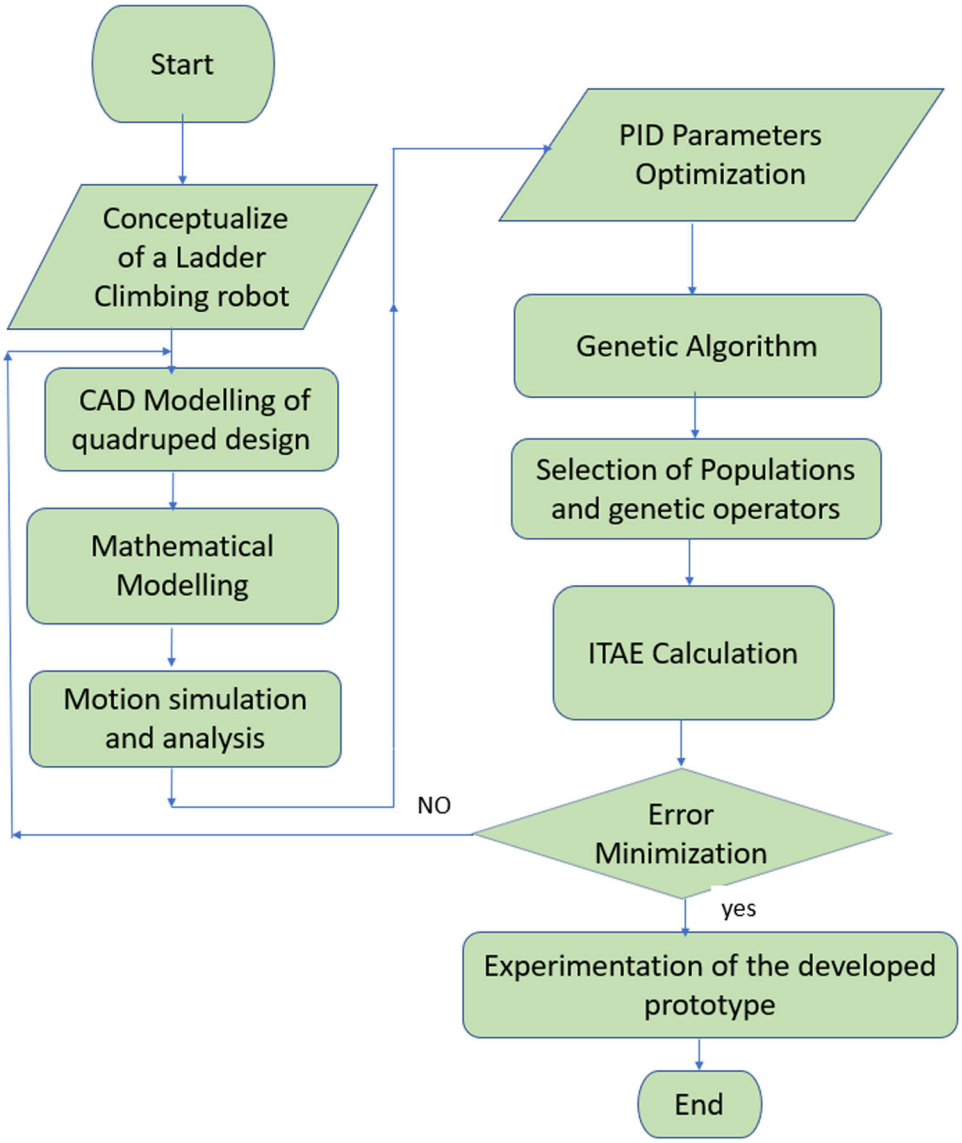

Fig. 2 The methodology adopted for the work

know the types of towers and varieties of ladders attached to the tower to conceptualize the robot and its dimensions. SubSect. 2.1 provides information on the types of towers and ladders attached to the tower. The design of robot and its working are included in SubSect. 2.2.

2.1 Types of towers and ladders

There are different varieties of telecom towers worldwide. Types of towers are shown in Fig. 3. The structural towers shown in Fig. 3a, b and d contain a ladder inside the structure of the tower. The ladder-climbing robot has to be accommodated in the narrow tower space at the top of the tower.

The robot is designed to climb a telecom tower, inspect the electronic equipment installed on the tower's top, and assist the rigger. The riggers climb the tower with a ladder attached to all the towers. The designed robot utilizes the existing ladder attached to the tower to climb. A survey of all types of ladders attached to the tower is carried out, and the dimensions of all ladders are collected. The two basic ladder varieties commonly used on telecommunications towers have been identified for deciding the robot's dimensions and motion. Figure 4 shows the types of ladders for the tower.

The ladder attached to the tower has a straight rung, as shown in Fig. 4a, and the zig-zag rung is shown in Fig. 4c. OSHA (Organizational Safety and Health Administration) has recommended the dimensions of the ladders. The regulations for telecom tower ladders indicate the dimensions of the ladder. One of them is shown in Fig. 4b.

(a) Ground-Based Tower (GBT), 3-Legged

(b) Ground-Based Tower (GBT), 4-Legged

(c) Ground-Based Mast (GBM)

(d) Roof Top Tower (RTT)

(e) Roof Top Pole (RTP)

Fig. 3 Different types of telecom towers exist worldwide [22] **a** ground-based tower (GBT), 3-Legged **b** ground-based tower (GBT), 4-legged **c** ground-based mast (GBM) **d** roof top tower (RTT) **e** roof top pole (RTP)

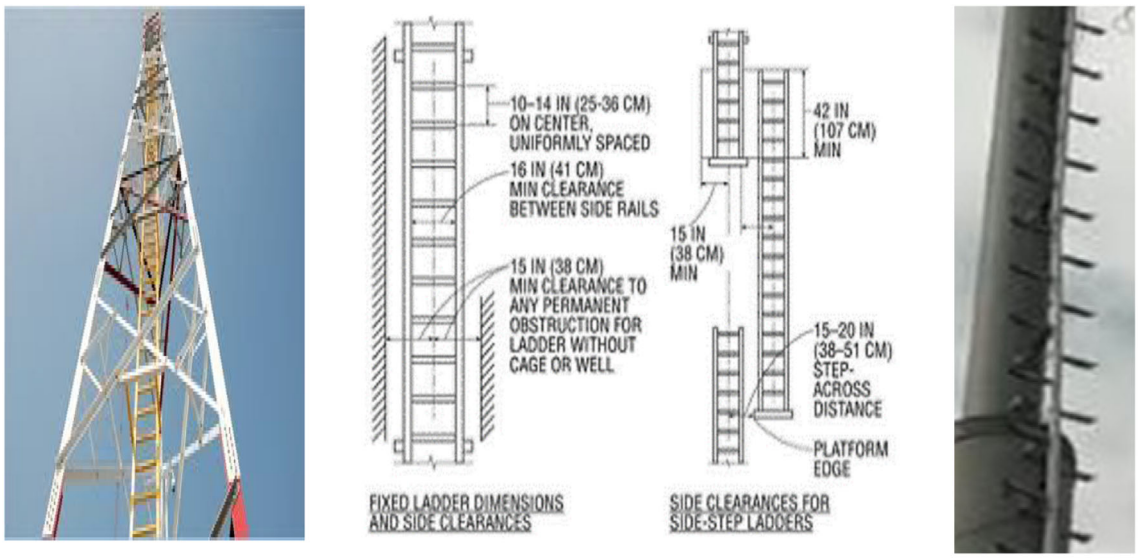

(a) The Ladder on a telecom tower for climbing [53], [54]

(b) Ladder Dimensions as per Regulations [55]

(c) Ladder on the real tower [40]

Fig. 4 The ladders on telecom towers for climbing **a** The ladder on a telecom tower for climbing [53, 54] **b** ladder dimensions as per regulations [55] **c** ladder on the real tower [40]

2.2 Design of the robot

The ladder dimensions are extremely useful for determining the dimensions of the proposed robot. As shown in Fig. 4b, the distance between two rungs ranges between 10–14 inches, i.e., 250–360 mm. A quadruped robot configuration is selected to design the mechanism capable of climbing the ladder, considering 300 mm rung distance. Each leg has three degrees of freedom, and all the joints are of revolute type chosen for the present application. Twelve degrees of freedom and a three-point contact climbing pattern are

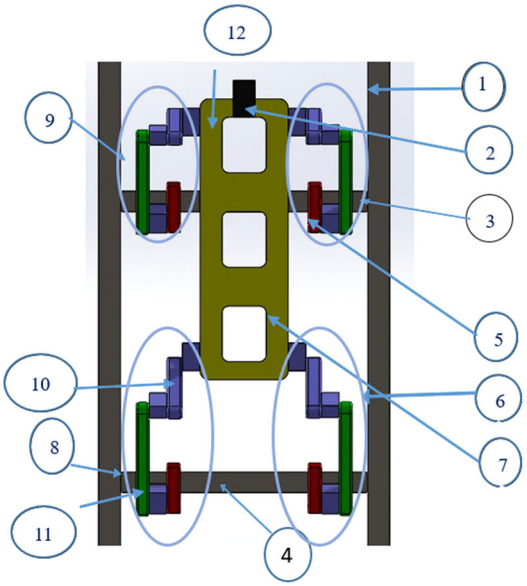

(a) Front view of the robot

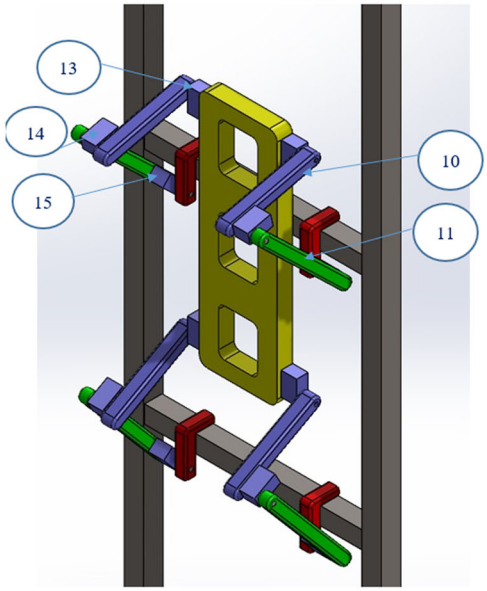

(b) Isometric View of the Robot

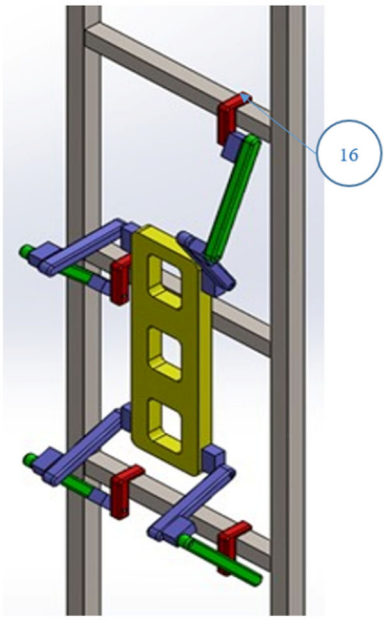

(c) Robot one leg actuated to move to next rung

Fig. 5 Proposed design of climbing robot **a** front view of the robot **b** isometric view of the robot **c** robot one leg actuated to move to next rung

considered for analysis. Figure 5 shows a CAD model of the proposed robot design, Fig. 5a represents the front view of the robot showing the majority of the parts, and Fig. 5b is a perspective view of the robot on the ladder in a static position, and Fig. 5c shows the Robot one leg motion up to the next rung. Table 1 shows the list of parts and corresponding part numbers.

The various components, such as grippers, links, and platforms, are designed in SolidWorks. The diagram description and work of the robot in Fig. 5 are as follows. The numbers written in parenthesis represent the robot's part numbers with reference to Fig. 5.A ladder-climbing robot (12) is used to climb the ladder (1), as shown in Fig. 5a. It has four legs; namely top right leg (3), lower right leg (6), lower left leg (8) and top left leg (9). Each leg has a gripper (5), with the help of which it establishes contact with the ladder rung (4). The robot's four legs are attached to the base plate (7). Each leg is made up of 3 links: link 1 (10), link 2(11) and gripper (5).

Table 1 List of components of the robot

References	Part name	References	Part name
[1]	Ladder	[9]	Upper left Leg
[2]	Camera	[10]	Link 1
[3]	Upper right Leg	[11]	Link 2
[4]	Ladder rung	[12]	Robot
[5]	Gripper	[13]	Motor1
[6]	Lower right Leg	[14]	Motor2
[7]	Base plate	[15]	Motor3
[8]	Lower left Leg	[16]	Gripper flat plate

As shown in Fig. 5b, motor 1 (13), motor 2 (14) and motor 3 (15) are used to operate link 1, link 2 and the gripper, respectively. The gripper is connected to the ladder rung with a flat plate (16), as shown in Fig. 5c.

The working of the robot to climb one rung on the ladder is mentioned below. The robot's four legs are identical; therefore, motion description is given for only one leg. All other legs follow the same sequence one by one, keeping three points of contact with the ladder all the time.

Position 1: (Static position) Fig. 5a shows the robot's static position, with all four grippers supported on the ladder rung.

Step 1: Gripper (5) of the upper right leg (3) starts moving according to the programmed sequence. Flat plate (16) opens and moves 90^0 as motor 3 (15) actuates.

Step 2: Motor 1(13)) actuates link 1, and extension of link1 uplifts the upper right leg towards the next rung on the ladder.

Step 3: Motor 2 (14) actuates, and the link2 extension allows the leg to reach the next rung on the ladder.

Step 4: Motor 3 (15) actuates, allowing the gripper to move the flat plate and establish contact with the next rung. Position 2 (see Fig. 5c).

Step 5: A force sensor senses the contact of the flat plate and ladder rung, and then only the motion sequence of the upper left leg takes place.

Similarly, the motion of the lower two legs follows the same sequence one by one, and the robot advances to the next rung. Motion simulation of the robot is presented in Sect. 3.4.

3 Analysis of the robot

The robot is required to be lightweight and cost-effective. The weight of the robot depends highly on the material used. SubSect. 3.1 compares the material generally used to make a robots and details. The proposed robot's components and weight properties are also discussed. SubSect. 3.2 includes the mathematical modelling and its forward and inverse kinematic analysis. Static analysis and Finite element analysis are included in SubSect. 3.3. Motion simulation and dynamic analysis included in SubSect. 3.4.

Table 2 Quantity of the parts

Sr.No	Part name	Quantity
1	Motors	12
2	Gripper	4
3	Link 1	4
4	Link 2	4
5	Base plate	1

3.1 Material characteristics and components of the robot

The basic components of the robot are the baseplate, link 1, link 2 and the gripper. The purpose of the gripper is to make contact with the ladder and provide the contact force. Each leg of the robot comprises link 1, link 2 and a gripper, having three degrees of freedom. This quadruped climbing robot has four identical legs and is mounted on the four corners of the base frame (Refer to Fig. 5). Table 2 gives the total number of components required for final assembly.

As each leg is identical, a quarter model can be used for design and analysis. The design of a robot for telecom tower climbing is done by taking into account the weight and strength of the robot. The choice of material determines the weight of the robot.The primary objective of the choice of materials is the desired strength with minimum cost without compromising the robot's performance. The choice of material must consider different properties such as strength, durability, weight, corrosion and heat resistance, and machinability. Table 3 shows the comparison between the different types of materials and their properties that can be used in the application of the climbing robot.

Based on the comparison table, plastic alloy ABS is preferable for making a quadruped climbing robot. It has significantly less mass density, which can offer lightweight and desired strength to the robot. Its material properties are as shown in Table 4.

An analysis of the robot is required to understand its motion parameters. Forward and inverse kinematics, along with dynamic analysis, are crucial for determining motion parameters and calculating actuator torque values. Dynamic analysis is based on the mass properties of each component. The material plastic alloys (ABS) is applied to the CAD model to obtain the mass property of all assembly components. The total weight of the robot is 1.6 kg, found based

Table 3 Comparison based on properties of various materials

Sr. No	Material	Mass density (kg/m^3)	Strength	Machining	Corrosion resistance	Applications
1	Plastic Alloy ABS (Acrylonitrile butadiene styrene)	1020	Medium	Poor	Fair	Automobile and building materials [56]
2	Plastic Acrylic	1200	Medium	Fair	Fair	Robotics, automobile sectors [57]
3	PLA (Polylactic Acid) Plastic	1250	Reasonably strong	Poor	Fair	Biodegradable medical devices [58]
4	Carbon Fiber-Hexcel	1790	Medium	Poor	Fair	Industrial applications [59]
5	Aluminum Alloy 7075	2810	High	Fair	Good	Aerospace application [60]
6	Aluminum Alloy 6061	2700	High	Fair	Good	Structural Applications [61]

Table 4 Material Properties ABS(Acrylonitrile butadiene styrene) [62]

Property	Value	Units
Mass density	1020	Kg/m^3
Elastic modulus	2×10^9	N/m^2
Tensile strength	3×10^7	N/m^2
Poisson's ratio	0.394	
Shear modulus	3189×10^5	N/m^2

on the connection lengths and inertia properties calculated in solid works. Mass properties results obtained from solid works are shown in Fig. 6.

3.2 Mathematical modelling

The mathematical model is prepared for the Quadruped robot for climbing vertical ladders kept at 90^0 attached to the telecommunications tower. Due to the symmetric design and four identical legs, the mathematical modelling for all four legs is also similar. A mathematical model includes kinematic modelling, which includes forward and inverse kinematics. All three degrees of freedom of the leg are of the revolute type, and its forward kinematic analysis is done considering mapping between the end-point transformation frames. The Frame assignment of the leg is described in Fig. 7.

The three-degree robotic arm kinematic model describes the position and orientation of the end effectors and the relationship between the joint variables. The derivatives of kinematic parameters deal with the mechanics of motion without considering the forces to follow the trajectory defined in the working space. The problem of Control of arms demands forward and inverse kinematic models. Consider the general notations as L_1 is the length of link 1, L_2 is the length of link 2, L_3 is Gripper length, θ_1 is the angle of L_1 with respect to X- axis, θ_2 is the angle of L_2 with respect to L_1, and θ_3 is the angle of L_3 with respect to L_2.

Forward Kinematic Modelling of one leg of a quadruped climbing robot is presented here. Figure 7 shows the frame assignment for three revolute joint legs of a robot. Its Denvit-Hartenberg representation is shown in Table 5. Direct kinematic analysis is carried out to arrive at a final point coordinate according to the length of the links and the angle [63]. Equations (1–3) show each link's transformation matrix and Eq. (4) indicates the end point placement matrix [64].

$$ {}^{0}\mathrm{T}_1(\boldsymbol{\theta}1) = \begin{bmatrix} c_1 & -s_1 & 0 & L_1c_1 \\ s_1 & c_1 & 0 & L_1s_1 \\ 0 & 0 & 1 & 0 \\ 0 & 0 & 0 & 1 \end{bmatrix} \tag{1} $$

$$ {}^{1}\mathrm{T}_2(\boldsymbol{\theta}2) = \begin{bmatrix} c_2 & -s_2 & 0 & L_2c_2 \\ s_2 & c_2 & 0 & L_2s_2 \\ 0 & 0 & 1 & 0 \\ 0 & 0 & 0 & 1 \end{bmatrix} \tag{2} $$

$$ {}^{2}\mathrm{T}_3(\boldsymbol{\theta}3) = \begin{bmatrix} c_3 & -s_3 & 0 & L_3c_3 \\ s_3 & c_3 & 0 & L_3s_3 \\ 0 & 0 & 1 & 0 \\ 0 & 0 & 0 & 1 \end{bmatrix} \tag{3} $$

The orientation and position of the {3} with reference to {0} is now obtained as,

Fig. 6 Mass properties of the robot derived from solid works model

Mass properties of Stair Climbing Robot Design New
Configuration: Default
Coordinate system: -- default --

Mass = 1621.57 grams

Total weld mass = 0.00 grams

Volume = 858936.67 cubic millimeters

Surface area = 198316.43 square millimeters

Center of mass: (millimeters)
X = -24.84
Y = -386.85
Z = 55.75

Principal axes of inertia and principal moments of inertia: (grams * square millimeters)
Taken at the center of mass.
Ix = (0.00, 1.00, 0.01) Px = 12110958.26
Iy = (-1.00, 0.00, 0.00) Py = 34426899.54
Iz = (0.00, -0.01, 1.00) Pz = 42305531.20

Moments of inertia: (grams * square millimeters)
Taken at the center of mass and aligned with the output coordinate system.
Lxx = 34426896.42 Lxy = 12998.71 Lxz = 6159.20
Lyx = 12998.71 Lyy = 12116178.30 Lyz = 396684.00
Lzx = 6159.20 Lzy = 396684.00 Lzz = 42300314.28

Moments of inertia: (grams * square millimeters)
Taken at the output coordinate system.
Ixx = 282137783.49 Ixy = 15597267.28 Ixz = -2239690.90
Iyx = 15597267.28 Iyy = 18156720.48 Iyz = -34574675.17
Izx = -2239690.90 Izy = -34574675.17 Izz = 285972293.19

Fig. 7 Frame assignment for three revolute joint leg

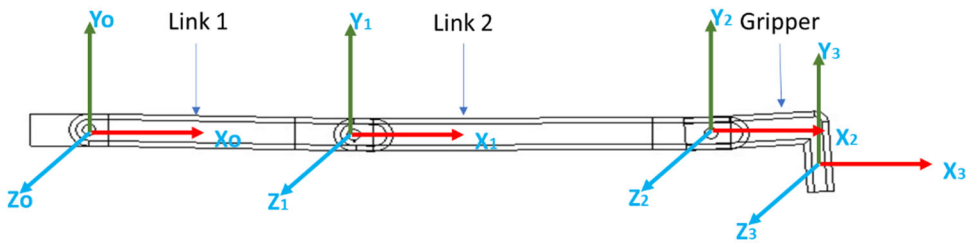

Table 5 D-H representation of a leg

Frame no	Link length	Link twist	Joint distance	Joint angle
0–1	L_1	0	0	θ_1
1–2	L_2	0	0	θ_2
2–3	L_3	0	0	θ_3

$^0T_3 = {}^0T_1 {}^1T_2 {}^2T_3$ which is shown in details as

$$^0T_3 = \begin{bmatrix} c_{123} & -s_{123} & 0 & L_3c_{123} + L_2c_{12} + L_1c_1 \\ s_{123} & c_{123} & 0 & L_3s_{123} + L_2s_{12} + L_1s_1 \\ 0 & 0 & 1 & 0 \\ 0 & 0 & 0 & 1 \end{bmatrix} \quad (4)$$

The forward motion of a robot leg is a very significant step. It provides the position of the gripping point corresponding to the joint parameters and the link. For different joint locations, the gripper point changes the position. Figure 8 represents the motion of links and gripper position. The trajectory and final configuration are obtained though inverse kinematics which is discussed in subsequent part of this section. The motor controls the joint angle and obtains the desired gripper position. To simulate the gripper location, the solution of the set of Eqs. (1–3) is programmed in MATLAB, and trajectory points of end-points of the links and gripper are plotted. The dotted line represents link L_1, L_2, and the gripper point variations with respect to an angle turned.

Inverse kinematics is also required for the link end-point. For a planer mechanism, the user gives the desired position (X, Y) and the total angle at the gripper as Φ, where $\Phi = \theta_1 + \theta_2 + \theta_3$. Based on that, the coordinates of the 1st link and 2nd link, and θ_1, θ_2, θ_3 can be obtained. Figure 9 shows the link and joint configuration of the leg of the climbing robot. From Fig. 9, Eq. (4) is used to solve inverse kinematic analysis, and the equations of joint parameters are obtained.

$$\begin{bmatrix} C_1C_{23} & -C_1S_{23} & S_1 & C_1(L_3C_{23} + L_2C_2 + L_1) \\ S_1C_{23} & -S_1S_{23} & -C_1 & S_1(L_3C_{23} + L_2C_2 + L_1) \\ S_{23} & C_{23} & 0 & L_3S_{23} + L_2S_2 \\ 0 & 0 & 0 & 1 \end{bmatrix} = \begin{bmatrix} r_{11} & r_{12} & r_{13} & r_{14} \\ r_{21} & r_{22} & r_{23} & r_{24} \\ r_{31} & r_{32} & r_{33} & r_{34} \\ 0 & 0 & 0 & 0 \end{bmatrix} \quad (5)$$

$$C_1(L_3C_{23} + L_2C_2 + L_1) = r_{14} \quad (6)$$

$$S_1(L_3C_{23} + L_2C_2 + L_1 = r_{24} \quad (7)$$

Dividing the Eq. (7) by (6),

$$\theta_1 = Atan2(r_{24}, r_{14}) \quad (8)$$

To evaluate joint parameters from Eq. 5 it is necessary to identify the set of equations that gives individual parameters in the Equation. An inverse transformation approach is adopted to arrive at an individual parameter set of equations.

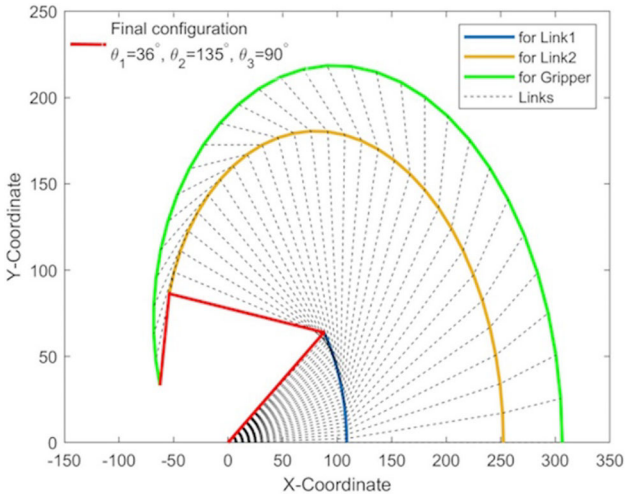

Fig. 8 End effectors location

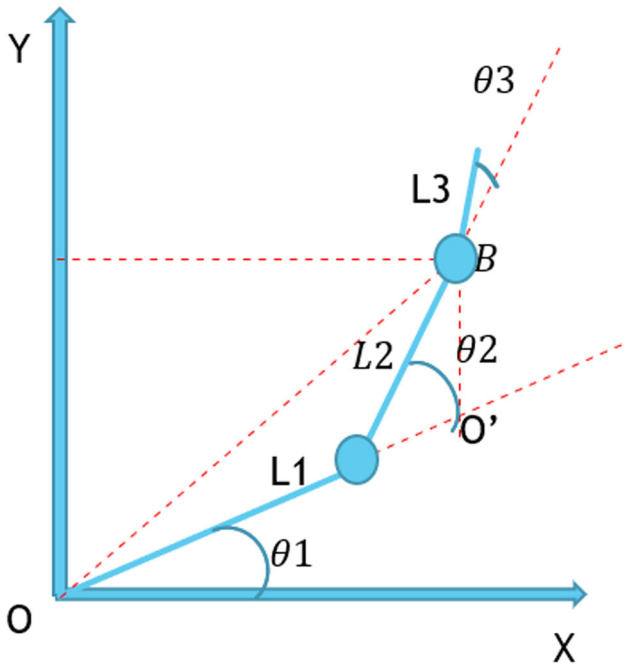

Fig. 9 Inverse kinematics leg positions

$$^2T_3 = \begin{bmatrix} C_3 & -S_3 & 0 & L_3C_3 \\ S_3 & C_3 & 0 & L_3S_3 \\ 0 & 0 & 1 & 0 \\ 0 & 0 & 0 & 1 \end{bmatrix}$$

$$\left[{}^2T_3\right]^{-1} = \begin{bmatrix} 2R3^T & 2R3^T2D3 \\ 000 & 1 \end{bmatrix}$$

$$L_2C_1C_2 = -L_3r_{11} + r_{14} \quad (9)$$

$$L_2S_1C_2 = -L_3r_{21} + r_{24} \tag{10}$$

$$L_2S_2 = -L_3r_{31} + r_{34} \tag{11}$$

By squaring Eqs. (9) and (10), and adding gives,

$$L_2^2C_2^2\left(C_1^2 + S_1^2\right) = (-L_3r_{11} + r_{14})^2 + (-L_3r_{21} + r_{24})^2$$

From this θ_1 is eliminated because $C_1^2 + S_1^2 = 1$, thus

$$L_2C_2 = \pm\sqrt{(-L_3r_{11} + r_{14})^2 + (-L_3r_{21} + r_{24})^2} \tag{12}$$

Dividing Eq. (11) by Eq. (12), gives

$$\frac{S_2}{C_2} = \frac{-L_3r_{31} + r_{34}}{\pm\sqrt{(-L_3r_{11} + r_{14})^2 + (-L_3r_{21} + r_{24})^2}}$$

$$\theta_2 = \text{Atan2}((-L_3r_{31} + r_{34}), \pm\sqrt{(-L_3r_{11} + r_{14})^2 + (-L_3r_{21} + r_{24})^2}\Big) \tag{13}$$

Now, $\frac{S_{23}}{C_{23}} = \frac{r_{31}}{r_{32}}$

$$\theta_2 + \theta_3 = \text{Atan2}(r_{31}, r_{32})$$

$$\theta_3 = \text{Atan2}(r_{31}, r_{32}) - \theta_2 \tag{14}$$

Equations (8,13,14) indicates the θ_1, θ_2 and θ_3 value obtained. It is important to mention that the inverse kinematics analysis results in two values of θ_1, as shown in Eq. (8). The Joint angle θ_1 lies either in quadrants 1 and 3 or in quadrants 2 and 4. Looking at the leg motion constraints, the results obtained in the 1st and 2nd quadrants are useful for joint angles for upward climbing motion. Similarly, θ_2 and θ_3 joint parameters are identified. It is necessary to mention that the gripper motion is restricted to 90^0 in open and closed situations.

3.3 Static and finite element analysis of a ladder-climbing robot

Static stability of the robot is to be maintained through the weight and reaction forces of clamps. Figure 10 shows that only two forces act on the robot when stationary on the ladder.

The first force is the robot's weight, acting in a downward direction because of gravitational pull. The second force is the normal reaction from the ladder at the robot's clamps (R1, R2, R3 and R4) acting upward. The total weight of the robot is 1.6 kg. The payload of 2 kg and factor of safety of 2 converts the total load to 8 kg. Considering Normal Reaction (N) at a particular leg contact,

$m * g = 4 * N;$

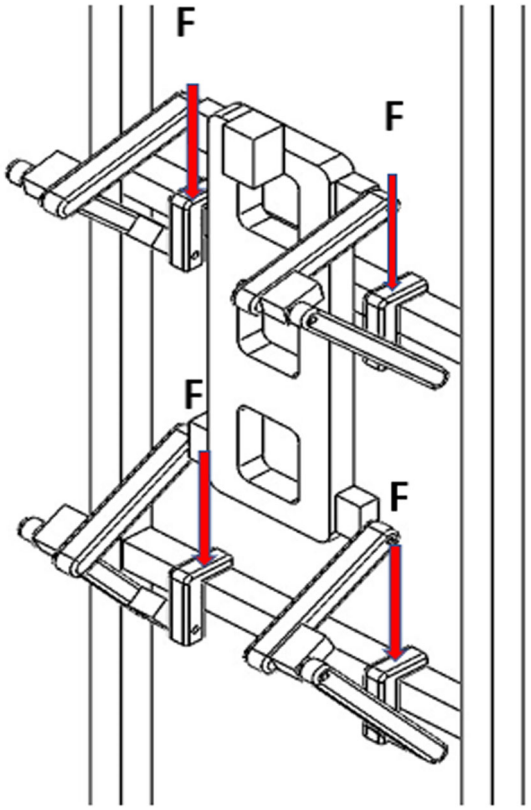

Fig. 10 Force on grippers

Therefore,

$$N = m * g/4 = 8 * 10/4 = 20 \text{ Newton}$$

To have static stability for the robot, all the reactions applied by the ladder on the robot at all contact surfaces must be greater than N. Hence,

$$R1, R2, R3, R4 \geq N \tag{15}$$

The necessary condition to be fulfilled to maintain the static stability of the robot on the ladder is given in Eq. (15).

The robot is designed to climb the telecommunication tower ladders and inspect the top of the tower at about 80 m height. The tower's cross-section becomes narrow at the top. The design of the robot is done considering the space available from the bottom to the top of the tower. The robot shall transport the inspection device and the load of tools to be transferred from bottom to top. The compact robot is built to withstand a load of up to 80 N. This load includes the self-weight of the Robot and Payload with a safety factor of 2. The payload of the robot is 2 kg, and self-weight of the plastic alloy robot is nearly 1.6 kg. In static structure analysis, load on each leg is considered as 20 N, i.e. distributing 80 N on each leg. The stress generated in the components are

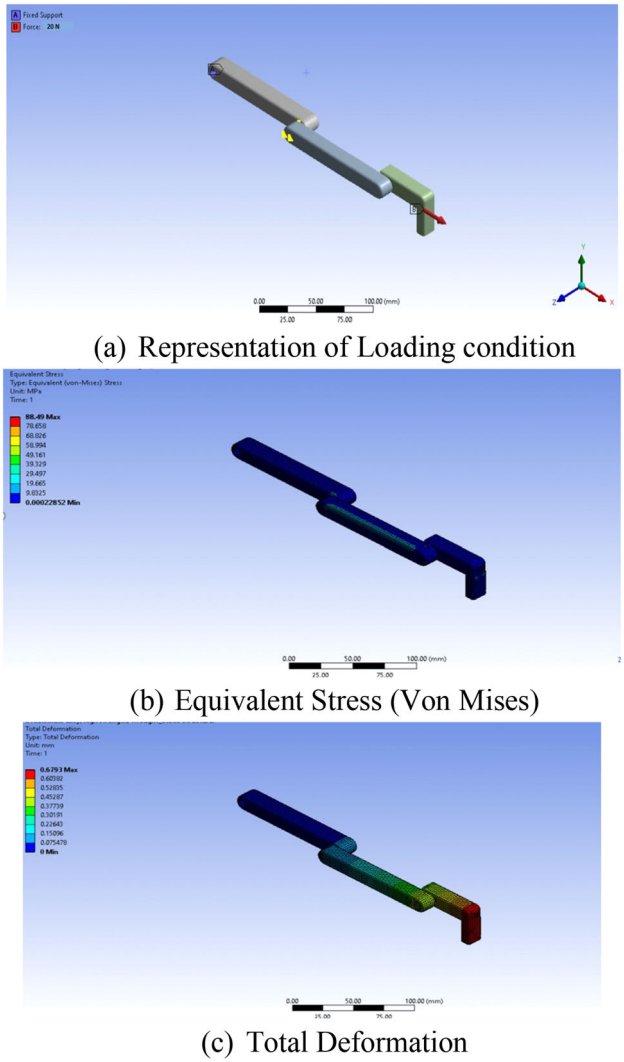

(a) Representation of Loading condition

(b) Equivalent Stress (Von Mises)

(c) Total Deformation

Fig. 11 Results of FEA analysis **a** representation of loading condition **b** Equivalent stress (Von Mises) **c** total deformation

identified by performing a finite element simulation on one leg of the robot considering the axis symmetry of the robot. The static structure and its stresses have been analysed in ANSYS, as shown in Fig. 11.

Figure 11a shows the loading condition of the gripper. The total load is distributed equally to all four grippers. The meshing is done by taking mixed-mode elements to cover the intricate shapes of the robot properly. Figure 11b shows the Von Mises stresses generated in the robot structure. That shows low-stress levels and that the designed robot is safe from the generated stress. Figure 11c represents the deformation of the robot. Results of the deformation analysis show

Table 6 Motion sequence for climbing motion of a robot

Sr. No	Time (in seconds)	Actuation	Motion
1	0–1	Pause	Pause
2	1–2	Gripper opens	Gripper lifts (90°)
3	2–3	Link 1	Extension
4	3–4	Link 2	Extension
5	4–5	Gripper holds the next rung	Rotation of gripper to hold rung

that the maximum deformation is 0.6 mm, which is also relatively small and admissible. It indicates that the designed robot has enough strength to perform a given task.

3.4 Motion simulation of a robot

As kinematic parameters like position, velocity, and acceleration are functions of a point, it is important to know their variation through the simulation study. Three points of contact are maintained with a ladder to maintain the robot's stability. Motion algorithm is required to design before simulation. Based on the sequential algorithm steps, the movement is applied in the motion study of solid works. The motion sequence adopted for the analysis is mentioned in Table 6.

Motion simulation of a ladder-climbing robot is shown in Fig. 12. Simulation is done using motion analysis in solid works. Maintaining contact with three legs with the ladder and having one leg gripper actuate at a time to advance the rung on the ladder is recommended. Each of the four legs is required to perform the same motion sequence. Thus, the time required to rise one step on the ladder is 20 s.

3.5 Dynamic analysis

Dynamic analysis of the leg of the climbing robot is presented in this section. It is important to use the proper capacity of the motors to drive the leg. Each joint consists of a servomotor to help the climbing robot advance steps on the ladder. The dynamic analysis results will be utilized to select the servo drives. The Dynamic analysis is performed to derive a mathematical model for torque τ. The velocity components are given in Eqs. (16), (17) and (18) [65]

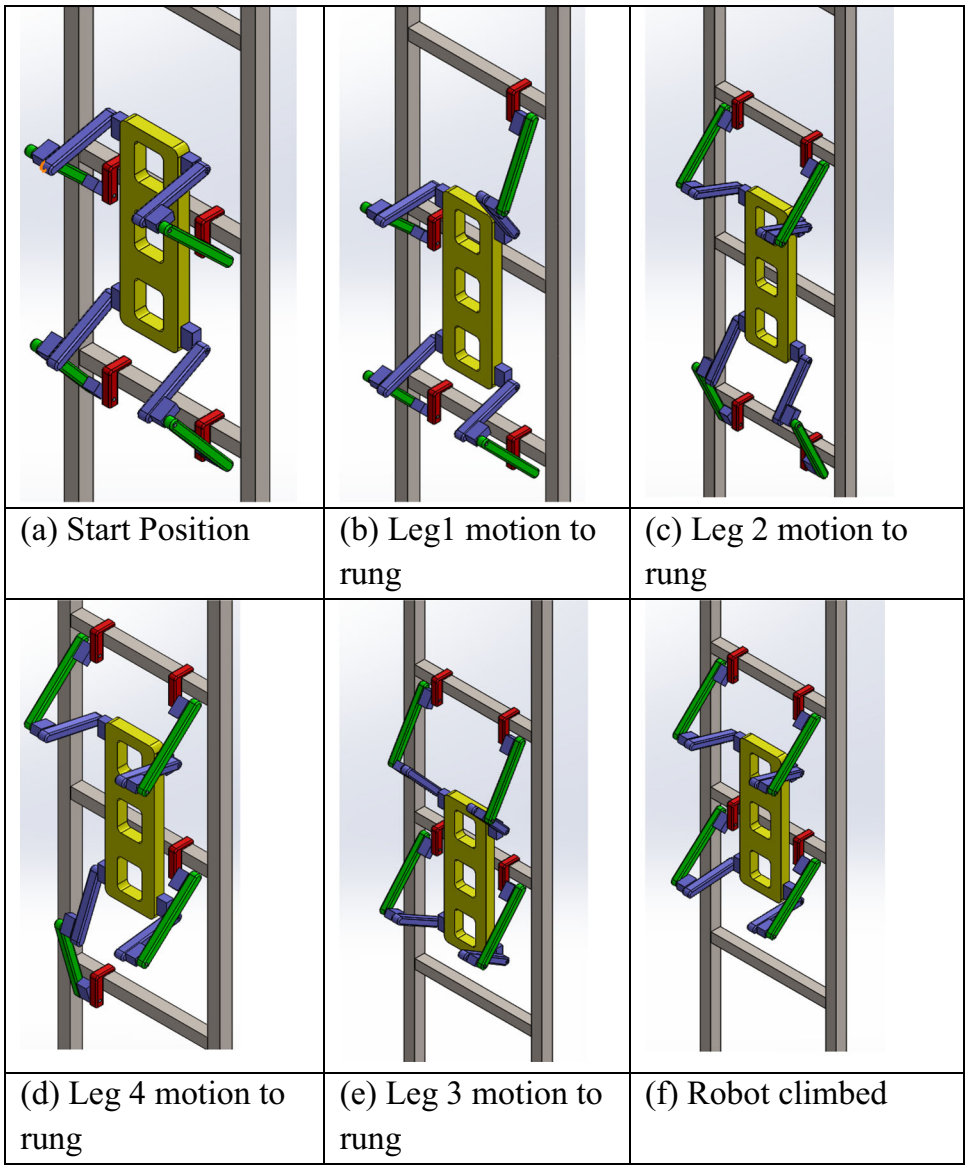

Fig. 12 Motion simulation of a robot **a** start position **b** Leg 1 motion to rung **c** Leg 2 motion to rung **d** Leg 4 motion to rung **e** Leg 3 motion to rung **f** robot climbed

$$\begin{bmatrix} \dot{X}_1 \\ \dot{Y}_1 \end{bmatrix} = \begin{bmatrix} -\sin\theta_1 * \dot{\theta}_1 \\ \cos\theta_1 * \dot{\theta}_1 \end{bmatrix} * (L_1) \tag{16}$$

$$\begin{bmatrix} \dot{X}_2 \\ \dot{Y}_2 \end{bmatrix} = \begin{bmatrix} -\sin\theta_1 * \dot{\theta}_1 - \sin(\theta_1 + \theta_2) * (\dot{\theta}_1 + \dot{\theta}_2) \\ \cos\theta_1 * \dot{\theta}_1 \cos(\theta_1 + \theta_2) * (\dot{\theta}_1 + \dot{\theta}_2) \end{bmatrix} * \begin{pmatrix} L_1 \\ L_2 \end{pmatrix} \tag{17}$$

$$\begin{bmatrix} \dot{X}_3 \\ \dot{Y}_3 \end{bmatrix} = \begin{bmatrix} -\sin\theta_1 * \dot{\theta}_1 - \sin(\theta_1 + \theta_2) * (\dot{\theta}_1 + \dot{\theta}_2) - \sin(\theta_1 + \theta_2 + \theta 3) * (\dot{\theta}_1 + \dot{\theta}_2 + \theta_3) \\ \cos\theta_1 * \dot{\theta}_1 \cos(\theta_1 + \theta_2) * (\dot{\theta}_1 + \dot{\theta}_2) \cos(\theta_1 + \theta_2 + \theta 3) * (\dot{\theta}_1 + \dot{\theta}_2 + \dot{\theta}_3) \end{bmatrix} * \begin{pmatrix} L_1 \\ L_2 \\ L_3 \end{pmatrix} \tag{18}$$

Total velocities for links and grippers are mentioned in Eq. (19), [65].

$$\begin{aligned} V_1(\text{ Link 1 velocity}) &= \sqrt{\left[\left(\dot{X}_1^2\right) + \left(\dot{Y}_1^2\right)\right]} \\ V_2(\text{ Link 2 velocity}) &= \sqrt{\left[\left(\dot{X}_2^2\right) + \left(\dot{Y}_2^2\right)\right]} \\ V_3(\text{ Gripper velocity}) &= \sqrt{\left[\left(\dot{X}_3^2\right) + \left(\dot{Y}_3^2\right)\right]} \end{aligned} \tag{19}$$

The above equations result in the theoretical values of the velocities. The velocity equations are plotted in MATLAB, and velocity variation with joint parameters is obtained, as shown in Fig. 13. The Maximum velocity from MATLAB results is 10,930 cm/sec.

To achieve the robot's smooth functioning, motion-controlling parameters must be optimized.

Torque calculations for all three actuators are given by Eq. (20) [65].

$$\begin{aligned}
&\text{Kinetic Energy} - K = \frac{1}{2} * M * V^2 \\
&\text{Potential Energy} - \text{P} = \text{M} * \text{G} * \text{Y} \\
&\text{Langrage L}(\theta,\ \dot{\theta}) = \sum_{i=1}^{n} (Ki - Pi) \qquad (i = 1,\ 2,\ 3) \\
&\text{Torque} - \tau_i = \frac{d}{dt}\left(\frac{dL}{d\dot{\theta}i}\right) - \frac{dL}{d\theta i} \qquad (i = 1,\ 2,\ 3)
\end{aligned} \tag{20}$$

The design of the robot is axis-symmetric, and the single-leg analysis can be performed. Kinematic and dynamic analysis is done, and the torque results of joints in each link of leg1 are obtained in MATLAB, as shown in Fig. 14. The joint angles used in calculations of velocities and torque is as per the trajectory shown in Fig. 8. The maximum torque obtained as negative which is 80.1148 N cm (clock-wise) at $\theta_1 = 21.46°$ in Link 1. At this instant, joint angle of Link 2 is $\theta_2 = 80.47°$ and Gripper is $\theta_3 = 53.65°$. From the Fig. 14, it is seen that the torque in Link 2 and Gripper is very less compared to Link 1 at this instant which results in higher loading on joint of Link 1 and subsequent maximum torque value. Knowing the torque exerted on each link is imperative to select the appropriate actuators. The framing of the specification of actuators and the subsequent selection of actuators are done based on values of torque and velocity are obtained from Eqs. (19) and (20) in MATLAB.

The variation of torque shows sudden motion variation. It results in jerky motion. Therefore, PID parameters like proportional, integral, and derivative gain are important for imparting smoothing considerations. The optimization of PID parameters is done using a genetic algorithm, which is presented in Sect. 4.

4 Optimization of PID controller parameters using genetic algorithm

The ladder climbing robot is designed and analyzed to climb ladders at 90° to the ground level. The smooth motion of the robot on the ladder is highly recommended. Maintaining the jerk-free motion of a robot on the ladder tunning of PID controller parameters is of the most importance [66–68]. Proportional, Derivative and Integral gain parameters tunning is done experimentally in the industry through a trial-and-error method. This article proposes a criterion based on a genetic algorithm to minimize the integral time absolute error, and optimization of proportional values is performed. The proposed design of the robot is a quadruped-axis symmetric model. It is considered to analyze a quarter model of the robot, as shown in Fig. 4. Each leg of the robot has three degrees of freedom, and its transfer functions are derived for PID controller analysis.

In the PID controller, the values of Kp (proportional gain), Ki (integral gain), and Kd (derivative gain) were determined through a tuning process to achieve the desired system performance.

Kp (Proportional Gain): The Kp value controls the response to the present error. A higher Kp value increases the system's responsiveness but can lead to overshooting and instability. The value of Kp was adjusted by gradually increasing it until the system responded quickly but without excessive overshoot.

Ki (Integral Gain): The Ki value addresses accumulated past errors, helping to eliminate any steady-state offset. A small value of Ki was chosen initially to prevent instability, and then it was fine-tuned to eliminate the steady-state error without introducing oscillations.

Kd (Derivative Gain): The Kd value reacts to the rate of change of the error, damping the system's response and reducing overshoot. Kd was gradually adjusted to achieve smooth and stable behavior by preventing rapid changes that could lead to instability or oscillations.

These values were obtained through a combination of trial-and-error tuning and, where possible, using empirical tuning methods like Ziegler-Nichols. The goal was to balance the trade-offs between responsiveness, stability, and accuracy. This iterative process ensured that the controller met the desired performance criteria for the system.

In the PID controller, the values of Kp (proportional gain), Ki (integral gain), and Kd (derivative gain) were optimized using a genetic algorithm (GA) to achieve optimal system performance.

Genetic Algorithm for Tuning: Instead of manual tuning, a genetic algorithm was employed to automatically find the optimal values for Kp, Ki, and Kd. The genetic algorithm works by simulating the process of natural selection, iterating through generations of candidate solutions (sets of Kp, Ki, and Kd values) and refining them based on their performance.

Fitness Function: A fitness function was defined to evaluate the performance of each candidate PID controller. The fitness function could include criteria like minimizing the error,

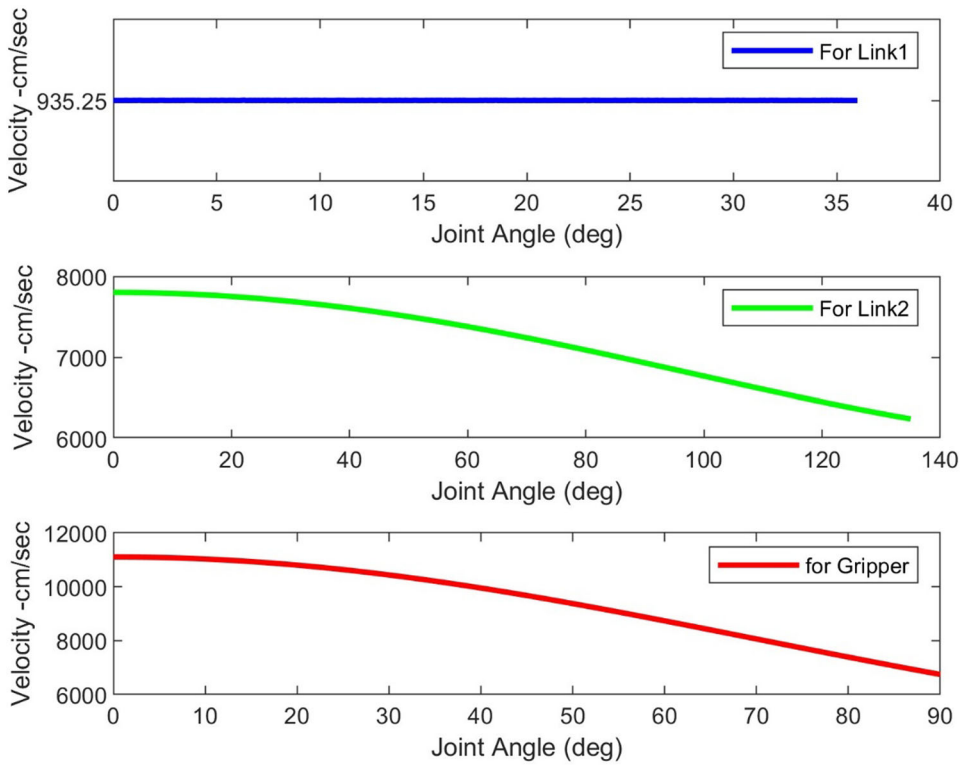

Fig. 13 Velocity variation of all links of leg 1 (MATLAB results)

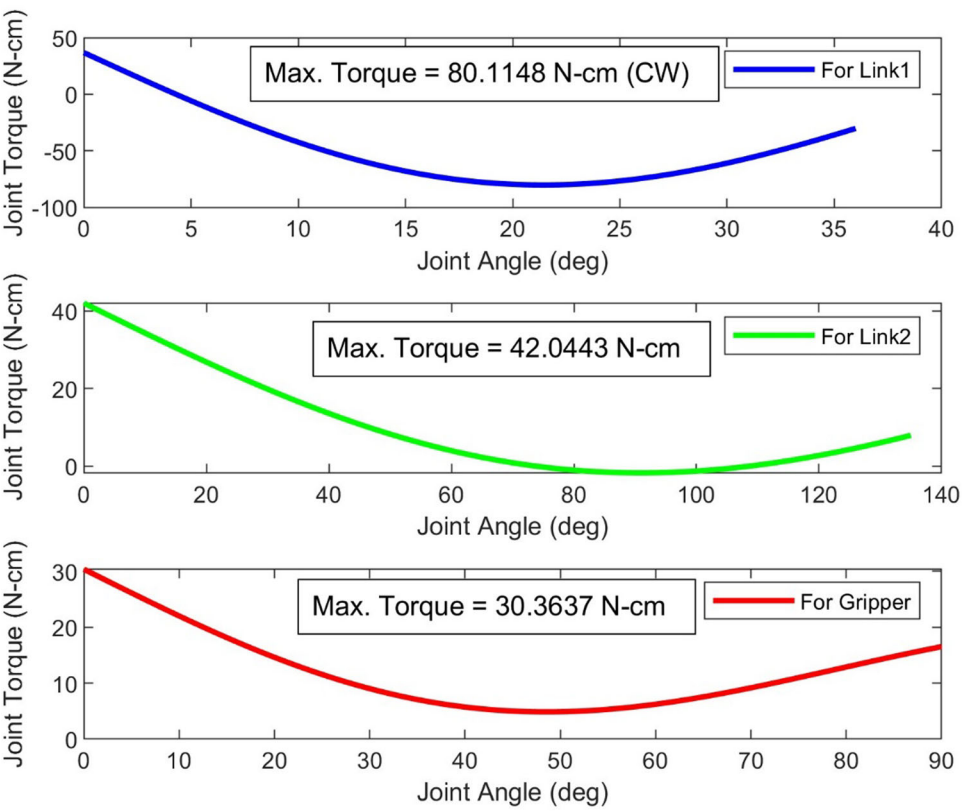

Fig. 14 Torque of all joints leg 1 (MATLAB results)

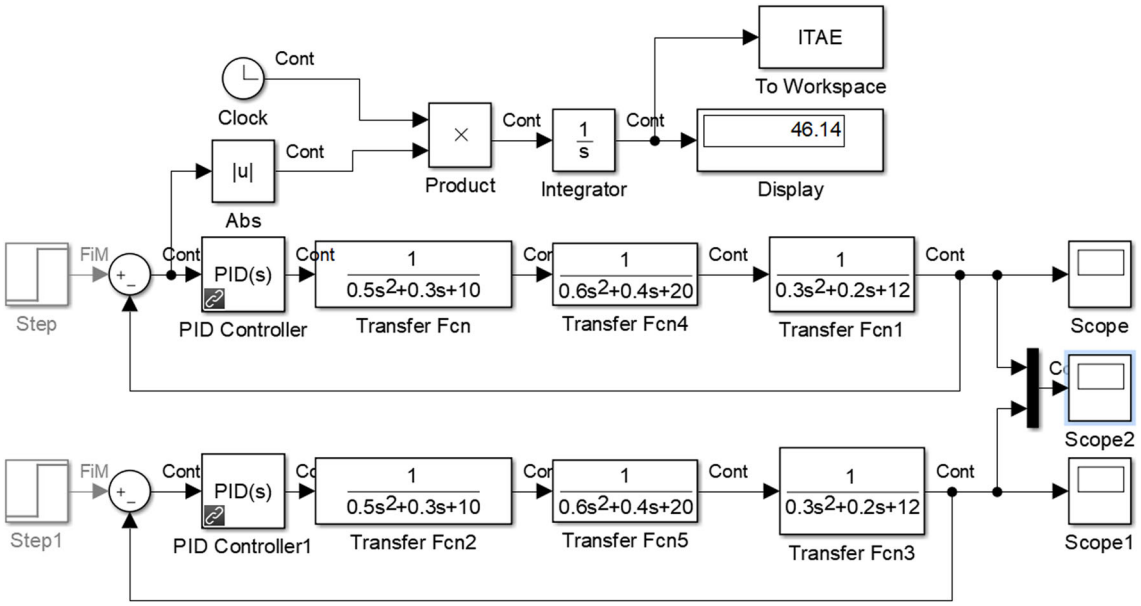

Fig. 15 Simulink model of the robot leg for PID controller tuning

reducing overshoot, improving settling time, and ensuring system stability. The algorithm explored different combinations of Kp, Ki, and Kd to minimize this fitness function.

Selection Process: Over successive generations, the genetic algorithm selected the best-performing candidates and applied genetic operators, such as crossover and mutation, to generate new sets of values. This process helped the algorithm converge toward an optimal solution, balancing system responsiveness, accuracy, and stability.

Final Values: The final values of Kp, Ki, and Kd were those that resulted in the best system performance according to the defined fitness criteria. This automated process ensures a more systematic and potentially more effective tuning than manual methods.

By using a genetic algorithm, we were able to efficiently and precisely determine the PID controller gains that provide the best overall system response.

Dynamic modelling of the robot is done considering the energy balance approach for each link of the robot leg. For the rotary motion of a link, its differential Equation of motion is derived as given in Eq. (21) using energy balance approach.

$$I_1\ddot{\theta_1} + C_1\dot{\theta_1} + K_1\theta_1 = T_1 \tag{21}$$

where I_1 = Mass moment of Inertia of the link, C_1 = Damping property of the material, and K_1 = Stiffness of the material. Applying the Laplas transformation approach, the transfer function of link 1, link 2, and link 3 are developed as follows.

$$\begin{aligned} Tf_1 &= \frac{\theta_1}{T_1(s)} = \frac{1}{I_1 s^2 + C_1 s + K_1} \\ Tf_2 &= \frac{\theta_2}{T_2(s)} = \frac{1}{I_2 s^2 + C_2 s + K_2} \\ Tf_3 &= \frac{\theta_3}{T_3(s)} = \frac{1}{I_3 s^2 + C_3 s + K_3} \end{aligned} \tag{22}$$

The derived transfer function of the system in Eq. (21) is simulated in Simulink, and the result is obtained against step input. An Evolutionary Genetic algorithm technique is used to solve the optimization problem. Genetic Algorithm provides robust and better solutions than other methods [69]. Fine-tuning of the PID controller parameters is required to make the robot climb a ladder with stability. The Simulink model of the system with PID controller and genetic algorithm integration is developed, as shown in Fig. 15, using derived transfer functions of the robot one leg. Simulation results for the optimized parameters are obtained, as shown in Fig. 16.

Identify a combination of the PID controller parameters such that the robot's resulting motion is stable and jerk-free while climbing the ladder. Transfer Function 1 indicates the motion described by link 1, Transfer Function 2 describes the motion of link 2 and Transfer Function 3 shows the motion of link 3. The transfer functions are plotted in series in Simulink, and the system response plot is achieved using the PID controller. The response shows a very high overshoot with periodic response. This indicates that it is required to choose values of an integral gain (k_i), proportional gain (k_p), and derivative gain (k_d) to arrive at an aperiodic (without

Table 7 Genetic algorithm parameters

Description	Selection of parameter
Fitness function	ITAE
Number of variables	3 (k_p, k_i, and k_d)
Lower bounds	[0 0 0]
Upper bounds	[100 100 100]
Population size	200
Selection criteria	Uniform
Fitness scaling function	Rank
Selection type	Tournament
Reproduction—crossover function	0.8 (Two points)
Mutation	0.05

overshoot) response to the system. The fitness function for the optimization considered is an integral time of the absolute error, as shown in Eq. (22) [70].

$$ITAE = \int_{t=0}^{t=final} |\Delta f| * t * dt \tag{23}$$

The genetic algorithm optimization process in the MATLAB optimization toolbox considers the following parameters. Table 7 highlights parameters considered for experimental trials for optimizations.

The total number of iterations conducted to arrive at the results is 100. The obtained optimized values of parameters are required to be inserted in the PID block of MATLAB Simulink, as shown in Fig. 16. It shows the schematic diagram of the system model integrated with ITAE (Integral Time Absolute Error). The bottom part of the diagram indicates the system's performance without optimization. The genetic algorithm is a metaheuristic technique inspired by natural selection based on an evolutionary algorithm [71]. The evolution usually starts from a population of randomly generated individuals and is an iterative process. Reproduction, crossover, and mutation are the stages required to be followed in each set of iterations to achieve better results. The obtained optimized values of parameters are needed to be inserted in the PID block of MATLAB Simulink.

The genetic algorithm is a metaheuristic technique inspired by natural selection based on an evolutionary algorithm. The evolution usually starts from a population of randomly generated individuals and is an iterative process. Reproduction, crossover, and mutation are the stages required to be followed in each set of iterations to achieve better results. The obtained optimized values of parameters are needed to be inserted in the PID block of MATLAB Simulink. The blue line in Fig. 16 indicates the system response with overshoot. The red line with optimized PID controller parameters k_p, k_i, and k_d results in smooth aperiodic motion, as shown in the red lines.

5 Development of a robot

The ladder climbing robot prototype is developed, and its experiments are conducted on the ladder. Figure 17 shows

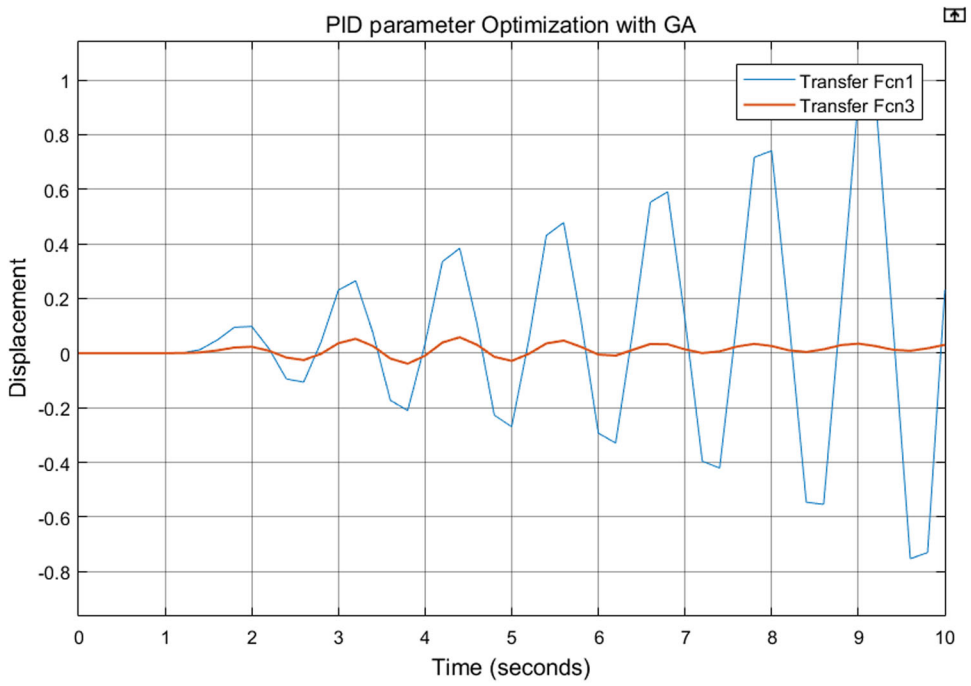

Fig. 16 Simulation results with and without Optimization of PID parameters

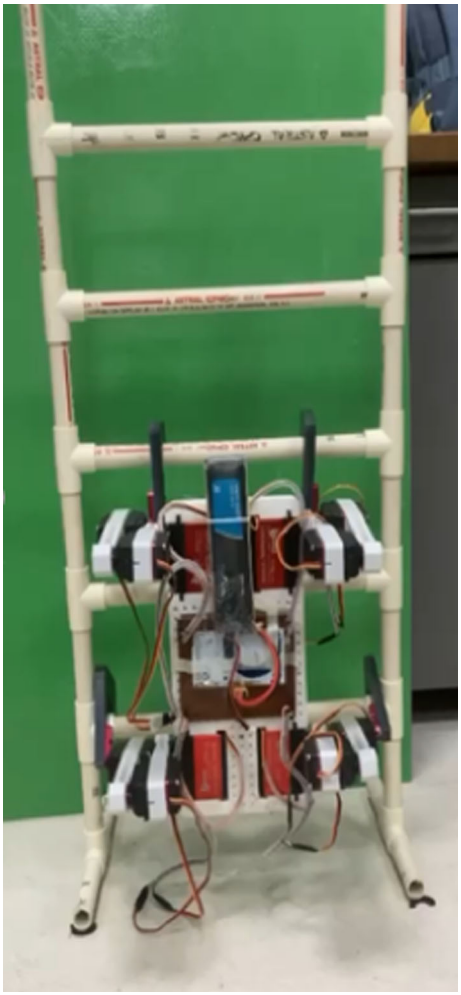

Fig. 17 Ladder climbing robot

the developed climbing robot with 12 servo motors, each with a capacity of 60 kg cm. The rated and working speed of the motor are 0.17 s/60°, and 0.13 s/ 60° respectively. It is controlled and programmed with Arduino Uno, with optimized PID controller parameters to get stable motion. It is designed to follow the programmed sequence built into the controller. A microcontroller is used to communicate with low-level components, and the microprocessor sends signals to the microcontroller based on the algorithm's decision. The robot uses the input signal from the antenna and decides the action.The robot design is a quadruped design, and it's a stable configuration as, at a time, only one leg actuates, and the other three legs maintain contact with the ladder. The robot's motion is dynamically stable as the centre of pressure falls within the support triangle. The motion sequence of the robot is indicated in Table 6. Figure 18 highlights the step-wise climbing of the robot on the ladder.

6 Conclusion

This study aimed to address the challenges faced by telecommunication companies in maintaining a vast network of towers, especially in reducing the risks associated with working at heights. A ladder-climbing robot prototype was developed to assist in telecom tower maintenance, providing a safer and more efficient alternative.

The research presented a comprehensive design and analysis of the robot, focusing on its kinematics, trajectory planning, and dynamic behavior. Forward and inverse kinematic analysis were successfully conducted to determine the robot's motion parameters, while trajectory planning ensured smooth climbing on the ladder.

Dynamic analysis provided insights into the forces and torques acting on the robot, which were crucial for selecting appropriate actuators. The results of these analyses were used to define the actuator specifications, leading to the selection of actuators that meet the system's operational requirements.

The PID controller parameters were optimized using a genetic algorithm, significantly improving the stability and performance of the robot during climbing. Simulation results demonstrated satisfactory motion and stability, confirming the robot's ability to perform the intended climbing task efficiently.

Additionally, the physical trials conducted on actual ladders validated the robot's design and control system, showing successful and stable climbing motion in real-world conditions. The successful trial indicates the potential of this robotic solution to be integrated into the telecom industry for safer and more effective tower maintenance.

In conclusion, this study not only developed a functional ladder-climbing robot but also provided a thorough analysis of its kinematics, dynamics, and control system. The results demonstrate that this robot can meet the demands of telecom tower maintenance, offering a viable solution to reduce the risks faced by workers and improve operational efficiency in the industry.

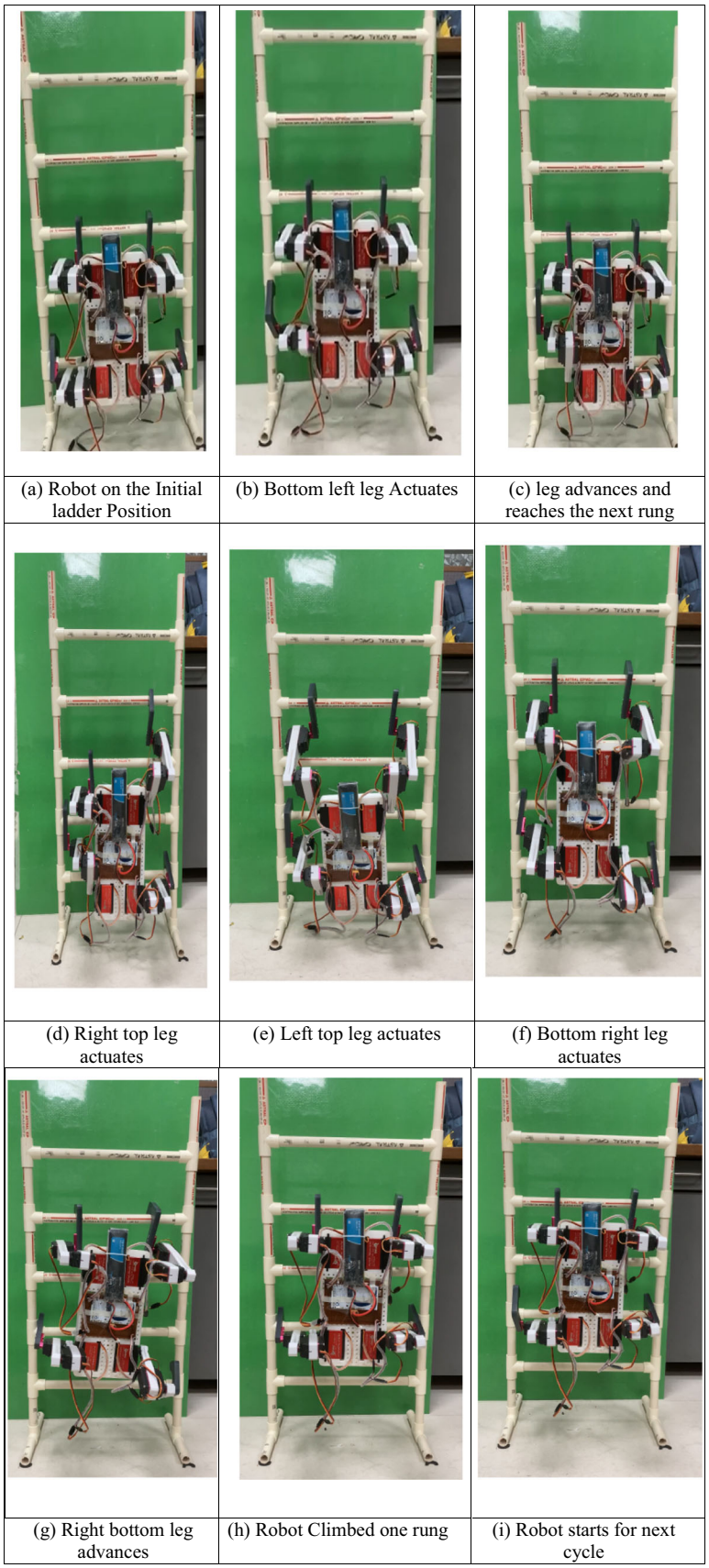

(a) Robot on the Initial ladder Position | (b) Bottom left leg Actuates | (c) leg advances and reaches the next rung

(d) Right top leg actuates | (e) Left top leg actuates | (f) Bottom right leg actuates

(g) Right bottom leg advances | (h) Robot Climbed one rung | (i) Robot starts for next cycle

Fig. 18 Climbing motion of the robot on the ladder **a** robot on the initial ladder position **b** bottom left leg actuates **c** leg advances and reaches the next rung **d** right top leg actuates **e** left top leg actuates **f** bottom right leg actuates **g** right bottom leg advances **h** robot climbed one rung **i** robot starts for next cycle

Supplementary Information The online version contains supplementary material available at https://doi.org/10.1007/s12008-024-02167-5.

Acknowledgements The Nirma University supported this work under Minor Research Project Grant [UID: IT/2022-23/01]. The authors sincerely thank the Institute of Technology, Nirma University, for its extended support.

References

1. Kamoun, F.: Toward best maintenance practices in communications network management. Int. J. Netw. Manag.Netw. Manag. **15**(5), 321–334 (2005). https://doi.org/10.1002/nem.576
2. N. Artical, The impact of COVID-19 on the global telecommunications industry. (2021). https://www.ifc.org/wps/wcm/connect/industry_ext_content/ifc_external_corporate_site/infrastructure/resources/covid-19+impact+on+the+global+telecommunications+industry.
3. Khan, M.K.: Importance of telecommunications in the times of COVID-19. Telecommun. Syst.. Syst. **76**(1), 1–2 (2021). https://doi.org/10.1007/s11235-020-00749-8
4. Joshi, H.: Indian Tower Industry The Future Is Data. Deloitte Touche Tohmatsu India Private Limited, (2021) https://www2.deloitte.com/in/en/pages/technology-media-and-telecommunications/articles/indian-tower-industry.html.
5. T. Company: Growth in tower companies globally. (2020). https://www.transparencymarketresearch.com/pressrelease/data-center-equipment-market.htm (Accessed Aug 18 2020).
6. G. Telecom, The new shape of the global telecom tower industry. (2020) https://www.towerxchange.com/the-new-shape-of-the-global-telecom-tower-industry/
7. Global Market Analysis: Global telecom tower market-industry analysis and forecast (2019–2027). (2019). https://www.maximizemarketresearch.com/market-report/global-telecom-tower-market/70701/ (Accessed Sep 30 2021).
8. Jang, E. et al.: Crowdsourcing rural network maintenance and repair via network messaging. In: Proceedings of the 2018 CHI Conference on human factors in computing systems pp. 1–12, (2018)
9. Shah, D., Dave, J., Majithiya, A., Patel, Y.: Conceptual design and analysis of pipe climbing robot. J. Phys. Conf. Ser. (2021). https://doi.org/10.1088/1742-6596/2115/1/012004
10. Shah, D., Dave, J., Detharia, D., Majithiya, A.: Design and analysis of the spray-painting robot for tall statues and monuments. J. Phys. Conf. Ser. (2021). https://doi.org/10.1088/1742-6596/2115/1/012003
11. Aljinovic, A., Crnjac, M., Nikola, G., Mladineo, M., Basic, A., Ivica, V.: Integration of the human-robot system in the learning factory assembly process. Proc. Manuf. **45**(2019), 158–163 (2020). https://doi.org/10.1016/j.promfg.2020.04.088
12. Zhang, X., Zhu, W., Wu, X., Song, T., Xie, Y., Zhao, H.: Dynamics and control for in-space assembly robots with large translational and rotational maneuvers. Acta Astronaut. Astronaut. **174**, 166–179 (2020). https://doi.org/10.1016/j.actaastro.2020.04.063
13. Ali, A.K., Lee, O.J., Song, H.: Robot-based facade spatial assembly optimization. J. Build. Eng. **33**, 101556 (2021). https://doi.org/10.1016/j.jobe.2020.101556
14. Gopinath, V., Johansen, K., Derelöv, M., Gustafsson, A., Axelsson, S.: Safe collaborative assembly on a a continuously moving line with large industrial robots. Robot. Comput. Integr. Manuf. **67**, 102048 (2021). https://doi.org/10.1016/j.rcim.2020.102048
15. Banta, H.D.: Effect of occupational safety and health on work productivity. In: Banta, H.D. (ed.) Anticipating and assessing health care technology, pp. 191–199. Springer, Netherlands, Dordrecht (1988)
16. Latif, S., Rana, R., Qadir, J., Ali, A., Imran, M.A., Shahzad, M.: Mobile health in the developing world : review of literature and lessons from a case study. IEEE Access **3536**, 1–16 (2017). https://doi.org/10.1109/ACCESS.2017.2710800
17. Andrew, T.N., Petkov, D.: The need for a systems thinking approach to the planning of rural telecommunications infrastructure. Telecomm. Policy **27**(1–2), 75–93 (2003). https://doi.org/10.1016/S0308-5961(02)00095-2
18. Lirov, Y., Yue, O.C.: Expert maintenance systems in telecommunication networks. J. Intell. Robot. Syst.Intell. Robot. Syst. **4**(4), 303–319 (1991). https://doi.org/10.1007/BF00314937
19. Mao, L., Li, Z., Zhang, D., Chen, J., Qi, J.: A distributed market-based boundary coverage algorithm for multiple microrobots with network connectivity maintenance. Adv. Robot. **27**(17), 1361–1373 (2013). https://doi.org/10.1080/01691864.2013.826422
20. Rosu, S.M., Rosu, L., Dragoi, G., Pavaloiu, I.B.: Risk Assessment of work accidents during the installation and maintenance of telecommunication networks. Environ. Eng. Manag. J.Manag. J. **14**(9), 2169–2176 (2018). https://doi.org/10.30638/eemj.2015.231
21. Alarcón, M. J., Zorzano, F. J., Jevtić, A., Andina, D.: Telecommunications network planning and maintenance. In: WMSCI 2008 - 12th World Multi-Conference Syst. Cybern. Informatics, Jointly with 14th Int. Conf. Inf. Syst. Anal. Synth. ISAS 2008 - Proc. 8: 64–68 (2008)
22. Shah, D., Dave, J.: A comprehensive review on deploying robotics application in telecom network tower's field maintenance: challenges with current practices and feasibility analysis for robotics implementation. J. Field Robot. **40**(7), 1860–1883 (2023). https://doi.org/10.1002/rob.22223
23. Tavakoli, M., Lopes, P., Sgrigna, L., Viegas, C.: Motion control of an omnidirectional climbing robot based on dead reckoning method. Mechatronics **30**, 94–106 (2015). https://doi.org/10.1016/j.mechatronics.2015.06.003
24. Ab Rashid, M.Z., Yakub, M.F., bin Shaikh Salim, S.A., Mamat, N., Putra, S.M., Roslan, S.A.: Modeling of the in-pipe inspection robot: A comprehensive review. Ocean Eng. **203**, 107206 (2020). https://doi.org/10.1016/j.oceaneng.2020.107206
25. Virgala, I., et al.: A snake robot for locomotion in a pipe using trapezium-like travelling wave. Mech. Mach. Theory (2021). https://doi.org/10.1016/j.mechmachtheory.2020.104221
26. Nishad, S.R., Halder, R., Banda, G., Thakur, A.: Development of a lizard-inspired wall-climbing robot using pressure sensitive adhesion. IEEE Access **10**, 72535–72544 (2022). https://doi.org/10.1109/ACCESS.2022.3189162
27. Seeja, G., Doss, A.S.A., Berlin Hency, V.: A survey on snake robot locomotion. IEEE Access **10**, 112100–112116 (2022). https://doi.org/10.1109/ACCESS.2022.3215162
28. Thakur, A.: Gait parameter tuning using bayesian optimisation for an alligator-inspired amphibious robot. Def. Sci. J. **73**(5), 519–530 (2023). https://doi.org/10.14429/DSJ.73.18315
29. Degallier, S., Righetti, L., Natale, L., Nori, F., Metta, G., Ijspeert, A.: A modular bio-inspired architecture for movement generation for the infant-like robot iCub. In: Proc. 2nd Bienn. IEEE/RAS-EMBS Int. Conf. Biomed. Robot. Biomechatronics, BioRob 2008 pp. 795–800 (2008)
30. Dubey, A.P., Pattnaik, S.M., Banerjee, A., Sarkar, R., Kumar, S.R.: Autonomous control and implementation of coconut tree climbing and harvesting robot. Proc. Comput. Sci. **85**, 755–766 (2016). https://doi.org/10.1016/j.procs.2016.05.263
31. Bisht, R.S., Pathak, P.M., Panigrahi, S.K.: Experimental investigations on permanent magnet based wheel mechanism for safe navigation of climbing robot. Proc. Comput. Sci. **133**, 377–384 (2018). https://doi.org/10.1016/j.procs.2018.07.046

32. Tavakoli, M., Marques, L., De Almeida, A.T.: 3DCLIMBER: climbing and manipulation over 3D structures. Mechatronics **21**(1), 48–62 (2011). https://doi.org/10.1016/j.mechatronics.2010.08.006
33. Liu, Y., Seo, T.W.: AnyClimb-II: dry-adhesive linkage-type climbing robot for uneven vertical surfaces. Mech. Mach. Theory **124**, 197–210 (2018). https://doi.org/10.1016/j.mechmachtheory.2018.02.010
34. Chen, W., Gu, S., Zhu, L., Zhang, H., Zhu, H., Guan, Y.: Representation of truss-style structures for autonomous climbing of biped pole-climbing robots. Rob. Auton. Syst. **101**, 126–137 (2018). https://doi.org/10.1016/j.robot.2018.01.002
35. Omoto, K., Doi, M., Ohtsuka, T.: Integrated optimization of climbing locomotion for a humanoid robot. IFAC-PapersOnLine **52**(16), 574–579 (2019). https://doi.org/10.1016/j.ifacol.2019.12.023
36. Moey, L.K., Teng, N.L.S., Ng, J.Y., Solihin, M.I., Badrulhisam, N.H.: Design and development of ladder climbing robot. Appl. Mech. Mater. **899**, 31–41 (2020). https://doi.org/10.4028/www.scientific.net/amm.899.31
37. Alkalla, M.G., Fanni, M.A., Mohamed, A.F.: Versatile climbing robot for vessels inspection. In: Proc. - 2015 Int. Conf. Control. Autom. Robot. ICCAR 2015 pp. 18–23 (2015) https://doi.org/10.1109/ICCAR.2015.7165995.
38. Alkalla, M. G., Fanni, M.A., Mohamed, A.M.: A novel propeller-type climbing robot for vessels inspection. In: IEEE/ASME Int. Conf. Adv. Intell. Mechatronics, AIM, pp. 1623–1628 (2015) https://doi.org/10.1109/AIM.2015.7222776.
39. Luk, B.L., Cooke, D.S., Galt, S., Collie, A.A., Chen, S.: Intelligent legged climbing service robot for remote maintenance applications in hazardous environments. Rob. Auton. Syst. **53**(2), 142–152 (2005). https://doi.org/10.1016/j.robot.2005.06.004
40. Dai, Y., Li, S., Rui, X., et al.: Review of key technologies of climbing robots. Front. Mech. Eng. **18**, 48 (2023). https://doi.org/10.1007/s11465-023-0764-0
41. Fang, Y., Wang, S., Cui, D., et al.: Design and optimization of wall-climbing robot impeller by genetic algorithm based on computational fluid dynamics and kriging model. Sci. Rep. **12**, 9571 (2021). https://doi.org/10.1038/s41598-022-13784-zNo
42. Borijindakul, P., Suthisomboon, T., Ji, A., et al.: Synergy between soft feet and an active tail to enhance the climbing ability of a bio-inspired climbing robot. Bionic Eng **21**, 729–773 (2024). https://doi.org/10.1007/s42235-023-00459-2
43. Wang, J., Jintao, W., Xiang, L., et al.: Wall-climbing robot system for volume calibration of large vertical storage tank. Mapan **38**(2), 295–306 (2023)
44. Fang, S., Shi, S., Wu, X., et al.: A walking and climbing quadruped robot capable of ground-wall transition: design, mobility analysis and gait planning. Intell. Serv. Robot.. Serv. Robot **16**, 431–451 (2023)
45. Saputra, A.A., Toda, Y., Takesue, N., Kubota, N.: A novel capabilities of quadruped robot moving through vertical ladder without handrail support. In: IEEE Int. Conf. Intell. Robot. Syst. pp. 1448–1453, (2019) https://doi.org/10.1109/IROS40897.2019.8968175.
46. Hashimoto, K. et al.: WAREC-1—a four-limbed robot having high locomotion ability with versatility in locomotion styles. In: SSRR 2017—15th IEEE Int. Symp. Safety, Secur. Rescue Robot. Conf. pp. 172–178 (2017) https://doi.org/10.1109/SSRR.2017.8088159.
47. Inoue, K., Fujii, S., Takubo, T., Mae, Y., Arai, T.: Ladder climbing method for the limb mechanism robot asterisk. Adv. Robot. **24**(11), 1557–1576 (2010). https://doi.org/10.1163/016918610X512596
48. Zhang, Y. et al.: Motion planning of ladder climbing for humanoid robots. In: IEEE Conf. Technol. Pract. Robot Appl. TePRA (2013) https://doi.org/10.1109/TePRA.2013.6556364.
49. Vaillant, J., et al.: Multi-contact vertical ladder climbing with an HRP-2 humanoid. Auton. Robots **40**(3), 561–580 (2016). https://doi.org/10.1007/s10514-016-9546-4
50. Bishop, R.H., Lathrop, R.C.: The optimal ITAE transfer functions for step input the optimal ITAE transfer functions for step input. **1**, pp. 5–7 (2018).
51. Utpat, L.S., Chavan, D.K., Yeolekar, N., Sahasrabudhe, A., Mandke, S.: Design optimization of robotic arms. Int. J. Eng. Res. Technol. **1**(3), 1–9 (2012)
52. Wen, J.T., Murphy, S.H.: PID control for robot manipulators. Control **23**(2), 386–391 (1990)
53. T. Types, "types of tower," 2007. http://www.steelintheair.com.au/Mobile-Phone-Tower.php
54. Telecom Tower Basics:, Cell phone tower basic. (2017). https://www.rfwireless-world.com/Tutorials/cell-phone-tower-basics-and-cell-phone-tower-types.html
55. O. Report Part 2, Osha report part 2. (2020). ttps://www.ishn.com/articles/110142-falls-structure-collapses-continue-to-claim-lives-in-comm-tower-industry (Accessed Aug 18, 2020).
56. A. Plastics Article, ABS plastics. Acrylonitrile butadiene styrene (ABS plastic): uses, properties & structure (specialchem.com) (2022) (Accessed Aug 23, 2022).
57. Article, Plastics material properties. Curbell, (2022). https://www.curbellplastics.com/resource-library/material-selection-tools/plastic-properties-table/ (Accessed Aug 23, 2022).
58. P. Biodegradeble, Plastics. 5 Types Of Biodegradable Plastics In 2024 - Almost Zero Waste. (2024) https://www.almostzerowaste.com/biodegradable-plastic-types Accessed June 22, 2024).
59. D. Sheet Hexcel, Carbon fiber. (2022). https://www.hexcel.com/user_area/content_media/raw/AS4C_Industrial_HexTow_DataSheet.pdf (Accessed Jun 12, 2022).
60. T. Article, Al-6061 properties strength and uses. Aluminum 6061, Al 6061-T6 alloy properties, density, tensile & yield strength, thermal conductivity, modulus of elasticity, welding (theworldmaterial.com) (2023) (accessed June 22, 2024).
61. T. W. Material, Aluminum 7075 Properties, 2023. https://www.theworldmaterial.com/al-7075-aluminum-alloy Accessed June 22, 2024).
62. Rahman, M.H., Alam, S.B., Das Mou, T., Uddin, M.F., Hasan, M.: A dynamic approach to low-cost design, development, and computational simulation of a 12DoF quadruped robot. Robotics (2023). https://doi.org/10.3390/robotics12010028
63. Mooney, J.G., Johnson, E.N.: A comparison of automatic nap-of-the-earth guidance strategies for helicopters. J. F. Robot. **33**(1), 1–17 (2014). https://doi.org/10.1002/rob
64. Q. Locomotion, No Title. (2015).
65. Roy, S.S.: Multi-body dynamic modeling of multi-legged robots. (2016).
66. Alvarez-Ramirez, J., Cervantes, I., Kelly, R.: PID regulation of robot manipulators: stability and performance. Syst. Control Lett. **41**(2), 73–83 (2000). https://doi.org/10.1016/S0167-6911(00)00038-4

67. Reyes, C., Gonzalez, F.: Mechanical design optimization of a walking robot leg using genetic algorithm. In: Climbing and Walking Robot: Proceedings of the 7th International Conference CLAWAR 2004, pp. 275–284, (2005) https://doi.org/10.1007/3-540-29461-9_25.
68. Martins, F.G.: Tuning PID controllers using the ITAE criterion. Int. J. Eng. Educ. **21**, 867–873 (2005)
69. Bhoskar, T., Kulkarni, O.K., Kulkarni, N.K., Patekar, S.L., Kakandikar, G.M., Nandedkar, V.M.: Genetic algorithm and its applications to mechanical engineering: a review. Mater. Today Proc. **2**(4–5), 2624–2630 (2015). https://doi.org/10.1016/j.matpr.2015.07.219
70. Bjorlykhaug, E., Egeland, O.: Mechanical design optimization of a 6DOF serial manipulator using genetic algorithm. IEEE Access **6**, 59087–59095 (2018). https://doi.org/10.1109/ACCESS.2018.2875272
71. Kouritem, S.A., Abouheaf, M.I., Nahas, N., Hassan, M.: A multi-objective optimization design of industrial robot arms. Alex. Eng. J. **61**(12), 12847–12867 (2022). https://doi.org/10.1016/j.aej.2022.06.052